

広島大学学術情報リポジトリ
Hiroshima University Institutional Repository

Title	Mesoporous Microspheres of Nickel-based Layered Hydroxides by Aerosol-Assisted Self-Assembly using Crystalline Nano-Building Blocks.
Author(s)	Tarutani, Naoki; Tokudome, Yasuaki; Jobbágy, Matías; Soler-Illia, Galo J. A. A.; Takahashi, Masahide
Citation	Journal of Sol-Gel Science and Technology , 89 : 216 - 224
Issue Date	2018-09-15
DOI	10.1007/s10971-018-4810-z
Self DOI	
URL	https://ir.lib.hiroshima-u.ac.jp/00053539
Right	<p>© The Author(s), under exclusive licence to Springer Science+Business Media, LLC, part of Springer Nature 2018 This version of the article has been accepted for publication, after peer review (when applicable) and is subject to Springer Nature's AM terms of use, but is not the Version of Record and does not reflect post-acceptance improvements, or any corrections. The Version of Record is available online at: https://doi.org/10.1007/s10971-018-4810-z This is not the published version. Please cite only the published version. この論文は出版社版ではありません。引用の際には出版社版をご確認、ご利用ください。</p>
Relation	



Mesoporous Microspheres of Nickel-based Layered Hydroxides by Aerosol-Assisted Self-Assembly using Crystalline Nano-Building Blocks.

Naoki Tarutani[†], Yasuaki Tokudome^{†*}, Matías Jobbágy[§], Galo J. A. A. Soler-Illia[#], Masahide Takahashi[†].

[†]Department of Materials Science, Graduate School of Engineering, Osaka Prefecture University, Sakai, Osaka 599-8531, Japan

[§] INQUIMAE-CONICET, Facultad Ciencias Exactas y Naturales, Universidad de Buenos Aires, Buenos Aires, C1428EHA, Argentina

[#] Instituto de Nanosistemas, Universidad Nacional de General San Martín-CONICET, Av. 25 de Mayo y Francia, San Martín, 1650, Argentina.

* Corresponding Author. Tel: (+81) 72-254-7598.

E-mail: tokudome@photomater.com

Abstract

Structural control in micro- and nanometer scale is necessary to design highly functional materials. Crystalline mesoporous microspheres are expected to improve electrochemical, catalytic, and adsorption performances. In this study, we focused on the preparation of templated mesoporous microspheres of nickel-based layered hydroxides by using pre-crystallized nano-building blocks (NBBs). Layered nickel hydroxide nanoparticles were prepared through an epoxide-mediated alkalization process and used as NBBs to construct microspheres. The spherical particles in micrometer scale were synthesized by ~~an spray-drying~~aerosol-assisted assembly of the NBBs dispersed in a solvent, in the presence of supramolecular templates. It was found that controlling the crystallization as well as the surface philicity permits to yield the NBB with an adequately small size and interparticle interactions that generate self-assembled mesoporous microspheres akin to those obtained in NBB-based mesoporous thin films. The preparation technique demonstrated here is highly versatile; templated mesoporous microspheres with various chemical compositions of nickel-based layered double hydroxides were successfully obtained.

Keywords

Crystalline mesoporous microspheres, nano-building blocks, layered nickel hydroxides, layered double hydroxides, epoxide-mediated alkalization

Introduction

The design and development of micro- and nanometer scale structures have attracted attention not only in fundamental aspects of materials science, but also in many applications. Mesoporous microspheres (MMSs) exhibit several unique/beneficial features which make them highly attractive for biomedical, sensing, photocatalytic and adsorbent applications [1-5]. The spherical shape of MMS improves the flowability of particles, the long term stability as suspensions,[6] and versatile processability for coatings. In addition, templated mesoporous structures of MMS provide a high specific surface area, large pore volume, and large number of accessible reactive surface sites, which enable them to be used as very efficient nano-reactors, and impart size selectivity of guest species due to high specific surface area, large pore volume, and well-defined regular pore size [7,8]. These features of MMS make them highly useful and attractive for applications, such as electrocatalysts and flow capacitors [9,10].

Although crystalline mesoporous materials are strongly demanded for applications, such as photocatalysts, capacitors, adsorbents [11,12], MMSs are generally obtained as amorphous materials showing lower performance compared to crystalline counterparts [13,14]. The crystallization of amorphous MMS preserving the original mesoporous structure is a considerable challenge. Post-treatments, such as heating, have been employed for the crystallization of MMS [15], however the crystallization of amorphous phases by post-treatments typically collapses mesoporous structures and disturbs micrometer-scale shapes in some cases. In addition, MMSs of non-oxide crystals, such as hydroxides, sulfides, and nitrides, are difficult to prepare through conventional methods due to the instability of these materials at high temperature in an air atmosphere. Alternative synthetic routes of the crystalline MMS are required toward a more versatile material design. One promising approach is the use of pre-formed nano-building blocks (NBBs) that can be self- and co-assembled with supramolecular templates [16-18].

We here demonstrate an approach using pre-crystallized NBBs for the fabrication of MMS materials with crystalline inorganic walls. Colloids of nanocrystalline layered nickel hydroxides, α -Ni(OH)₂, were prepared through an epoxide-mediated alkalization, in the presence of carboxylic acids. The resultant colloidal nanocrystals were used as NBBs to construct MMS through an aerosol assisted self-assembly process using a spray-dryer [19]. It was found that controlling the crystallization as well as the surface philicity permits to yield the NBB with an adequately small size and interparticle interactions that generate self-assembled mesoporous microspheres. The preparation technique demonstrated here is highly versatile and mesoporous microspheres of various chemical compositions of layered double hydroxides (LDHs), with tunable diameter, and shapes, were successfully designed.

Experimental

Chemicals.

Aluminum chloride hexahydrate ($\text{AlCl}_3 \cdot 6\text{H}_2\text{O}$, 98.0%), chromium(III) chloride hexahydrate ($\text{CrCl}_3 \cdot 6\text{H}_2\text{O}$, 99.5%), manganese(II) chloride tetrahydrate ($\text{MnCl}_2 \cdot 4\text{H}_2\text{O}$, 99.0%), iron(III) chloride hexahydrate ($\text{FeCl}_3 \cdot 6\text{H}_2\text{O}$, 99%), cobalt chloride hexahydrate ($\text{CoCl}_2 \cdot 6\text{H}_2\text{O}$, 99.0%), nickel chloride hexahydrate ($\text{NiCl}_2 \cdot 6\text{H}_2\text{O}$, 98.0%), copper chloride dihydrate ($\text{CuCl}_2 \cdot 2\text{H}_2\text{O}$, 99.0%), acrylic acid (99%), glutaric acid (98%), ethanol (99.5%), propylene oxide (> 99%), and Pluronic F127 block copolymer (F127) were used as received. Acrylic acid, propylene oxide, and F127 were purchased from Sigma-Aldrich Co. All other reagents were purchased from Wako Pure Chemicals Industries, Ltd. Ultrapure water of 18.2 $\text{M}\Omega \cdot \text{cm}$ resistivity was used in all experiments.

Synthesis of $\alpha\text{-Ni}(\text{OH})_2$ Mesoporous Microspheres.

$\text{NiCl}_2 \cdot 6\text{H}_2\text{O}$ (0.5 mmol) and glutaric acid (0.5 mmol) were dissolved in ethanol (17.2 mmol), and propylene oxide (7.5 mmol) was added to this solution under stirring. After stirring for 30 s, the solution was left at 25 °C for 1–8 min. The reacting solution was diluted with 50 mL of water dissolving F127 (2.5–15 μmol) and stirred for 1 min. The obtained homogenous sol was spray-dried using a Buchi B-290 mini spray-dryer. The spray conditions are as follows; inlet air temperature of 150 °C, gas (air, 35±5 RH%) flow rate of 246–742 L/h, peristaltic pump speed of 6 mL/min. The dried powders were collected from a sample glass vessel and heat treated at 250 °C for 6 h with a ramp rate of 1 °C/min under an air atmosphere.

Synthesis of Ni-M LDHs (M = Mn(II), Co(II), Cu(II), Al(III), Fe(III), and Cr(III)) Mesoporous Microspheres.

$\text{NiCl}_2 \cdot 6\text{H}_2\text{O}$ (0.375 mmol), $\text{MCl}_m \cdot n\text{H}_2\text{O}$ (M = Mn(II), Co(II), Cu(II), Al(III), Fe(III), Cr(III), $m = 2-3$, and $n = 2-6$) (0.125 mmol), and acrylic acid (1.0 mmol) were dissolved in ethanol (17.2 mmol), and propylene oxide (7.5 mmol) was added to this solution under stirring. After stirring for 30 s, the solution was left to stand at 25 °C for 60 min. The reacting solution was diluted with 50 mL of water dissolving F127 (2.5 μmol) and stirred for 1 min. The obtained homogenous sol was spray-dried with conditions of inlet air temperature of 150 °C, gas (air, 35±5 RH%) flow rate of 473 L/h, peristaltic pump speed of 6 mL/min. The dried powders were collected from a sample glass vessel and heat treated at 250 °C for 6 h with a ramp rate of

1 °C/min under an air atmosphere. The sample prepared through this process were described as Ni-M, where M is incorporated metal element (M = Mn, Co, Cu, Al, Fe, and Cr).

Characterization.

A scanning electron microscope (SEM) was employed to observe the morphologies and measure the diameter of the obtained MMSs (D_p). A transmission electron microscope (TEM; JEM-2000FX) and scanning TEM (STEM; JEM-2100F, JEOL, Japan) equipped with energy-dispersive spectroscopy (EDS) was employed at an operating voltage of 200 kV to measure the diameter of NBB (D_{NBB}) and to observe the mesostructures of the MMSs. Powder X-ray diffraction (PXRD) using Cu K α radiation ($\lambda = 0.1544$ nm) was used to characterize the crystalline phases. Small angle X-ray scattering (SAXS) measurement was performed to characterize the diameter and mesostructures of MMSs with a lab-scale diffractometer (SmartLab, Rigaku, Japan) and the beamline of the Brazilian Synchrotron Light Laboratory (LNLS, Brazil D11A-SAXS1-18927). Details of the analyses of SAXS data are explicit in the Supporting Information.

Results and discussion

Preparation α -Ni(OH) $_2$ NBB colloids for a Synthesis of Mesoporous Microspheres.

A solution containing nickel chloride and glutaric acid was used as a precursor solution; subsequent addition of propylene oxide induces alkalization in the solution [20]. Figure 1 shows the time-dependent change of relative ~~free-residual~~ Ni ion amount and particle diameter after the addition of propylene oxide. Along with reaction time, nanometer-sized particles formed and grew through the consumption of Ni ion, and gelation took place in 10 min. A homogenous pH increase in minute-scale induces a high degree of supersaturation condition, which leads to the massive formation of nuclei and the subsequent growth of hydroxide nanocrystals [21]. Single-nm-sized particles can be obtained within 5 min of reaction. As we reported previously [22], coordination of carboxylic acid to metal ions inhibits extensive crystal growth. For the proper self-assembly of block copolymer templates and NBBs toward mesoporous structure, NBBs are required to be smaller than the mesostructures (generally < 10 nm), narrow in size distribution, and highly dispersible in hydrophilic solvents [23-26].

The reaction time, t , of 2 min was chosen as a condition to prepare MMS because D_{NBB} of 3.1 nm at $t = 2$ min (Figure 1) is expected to be small enough for mesostructure formation. The PXRD pattern of spray-dried powder prepared from a solution of $t = 2$ min showed several sharp peaks assigned to remnant (unreacted) NiCl $_2$ ·2H $_2$ O and F127 [27] (Figure 2a). Coarse NiCl $_2$ ·2H $_2$ O crystals (crystallite size: 21 nm) was formed during drying because a large amount (91%) of Ni ion remained in solution at $t = 2$ min. In addition, the segregation of crystalline F127 took place during the spray-drying in spite of that the

concentration of F127 was the same as that reported for conventional synthesis of mesoporous materials [28]. This may be explained by relatively weak interaction of NBB with F127 compared with molecular precursors, such as alkoxides, as a result, macro-scale phase separation between NBB and F127 took place. In order to inhibit the segregation of coarse $\text{NiCl}_2 \cdot 2\text{H}_2\text{O}$ crystals and F127, reaction time and F127/Ni was tuned (See table in Figure 2). Along with increasing t , Ni ion was consumed (Figure 1) and the formation of $\text{NiCl}_2 \cdot 2\text{H}_2\text{O}$ phase was minimized. The segregation of F127 was prevented by reducing the F127/Ni ratio. At $t = 5$ min and F127/Ni = 0.005, spray-dried MMS shows PXRD pattern with broad peak around at $2\theta = 10^\circ$, corresponding to the 001 plane of glutarate-intercalated $\alpha\text{-Ni}(\text{OH})_2$ (9.0 Å) [22] (Figure 2b). The $\alpha\text{-Ni}(\text{OH})_2$ NBB colloids prepared under this condition were then diluted with aqueous media (used for spray-drying) and dropped on a TEM grid for their inspection (Figure 3a). The spray-dried MMS showed spheroidal shape with D_p of 0.808 μm , with a standard deviation of 0.196 μm (Figure 3b). The large standard deviation indicates a polydispersed distribution of particle diameter, which is a typical feature of spray-dried particles [28]. The NBBs composing MMS are smaller than wall thickness of typical F127 templated mesoporous structures [29,30], allowing co-assembly of the NBBs and F127 micelles (Figure 3c). The MMS were then heat-treated at 250 °C for 6 h to remove template F127. The PXRD pattern and SEM image of heat-treated MMS are comparable to those of original as-spray-dried MMS (Figure S1), which reveals that the resultant $\alpha\text{-Ni}(\text{OH})_2$ MMS was thermally-stable enough to allow the removal of the F127 template. The SAXS pattern of heat-treated MMS shows a peak centered at 0.384 nm^{-1} corresponding to a pore-to-pore periodicity of 16.4 nm (Figure 4a). TEM image of heat-treated MMS shows a wormhole-like mesoporous structure (Figure 4b) [31], which confirms again that the meso-scale structure is robust enough toward the heat-treatment. The present process is highly reproducible; the dilution of NBBs with 50 mL of water successfully quenched the growth and aggregation of NBBs, allowing the reproducible formation of mesoporous microspheres by spray-drying. SEM images of spray-dried MMS prepared at different quenching times, t_q , of 1 min and 3 h (duration time since diluting until spray-drying) are shown in Figure 5a and 5b. Microspheres were formed independent of t_q . SAXS patterns of spray-dried MMS prepared at $t_q = 1$ min and 3 h showed a comparable peak, suggesting the formation of comparable meso-periodicity. These results confirm that the diluting process could quench the growth of NBBs to form highly stable NBBs which assures the reproducibility of the spray-drying step; microspheres with comparable size and shape in μm , with comparable meso-periodic structure in nm were formed irrespective of t_q . Such a stable NBB colloid is highly preferable for a large scale continuous synthesis by spray-drying.

Diameter and shape control of $\alpha\text{-Ni}(\text{OH})_2$ Mesoporous Microspheres.

The controllability of diameter, size distribution and shape of MMS is known to be important for its practical applications, for example, tuning the rheological property of suspension toward specific applications [32,33]. The gas flow rate of spray-drying was varied in the range of 246–742 L/h to tune the diameter and shape of microspheres. SEM images (Figure 6a and 6b) show that D_p increased with decreasing flow rate. Generally, the diameter of sprayed droplets increased with decreasing flow rate, which leads to increasing the resultant D_p . The spray-dried MMSs showed a dimple pattern on their surfaces. If the diameter of sprayed droplets exceeds a critical value, the surface solidifies before the completion of evaporation of inner solvent, and the dimple pattern forms as a result of buckling induced by the shrinkage of the inner part upon drying. Particle size distributions of MMSs prepared with different gas flow rates are shown in Figure 6c. Along with the decrease of gas flow rate, D_p were indeed increased from $0.808 \pm 0.196 \mu\text{m}$ to $1.49 \pm 0.261 \mu\text{m}$ (Figure 6c inset). In conclusion, a variety of MMSs with controllable diameter and surface structure can be prepared by simply changing the spray-drying conditions.

Synthesis of Ni-M LDHs (M = Mn(II), Co(II), Cu(II), Al(III), Fe(III), and Cr(III)) Mesoporous Microspheres.

As described above, the reaction time, t and the F127/Ni ratio are essential parameters to obtain crystalline MMSs. The choice of carboxylic acid used as an additive is another important parameter to improve the dispersibility of NBBs. Systematic investigation revealed that using acrylic acid instead of glutaric acid is highly effective to prevent aggregation of growing NBB during the massive consumption of Ni(II) ions. In the case of acrylic acid used, 96.2% of precursor Ni(II) ions were consumed at $t = 60$ min without involving gelation, which is a preferable condition for the preparation of crystalline mesoporous materials through the present NBB approach. The PXRD pattern of spray-dried MMS was assigned to acrylate intercalated α -Ni(OH)₂ (Figure 7a) (lattice spacing: 12.3 Å) without segregation of other impurity phases [34]. The STEM image of NBB used for spray-drying ($t = 60$ min) was shown in Figure 7b. The D_{NBB} was 2.00 nm which is small enough to form F127 templated mesoporous structures. The colloid of NBB prepared with acrylic acid was spray-dried to prepare MMS. SEM and TEM observations of the spray-dried MMS after heat-treatment at 250 °C for 6 h reveals that the microspheres have smooth surface while a templated mesoporous structure was formed inside the microspheres (Figure 7c and 7d).

The precursor nickel chloride was partially replaced with a metal chloride of a target element, in order to tune the chemical composition of spray-dried MMSs. The PXRD patterns of spray-dried MMSs with various chemical compositions are shown in Figure 8a. All of the patterns were comparable to that of acrylate intercalated α -Ni(OH)₂, suggesting the formation of layered hydroxides. Figures 8b and c show STEM images of Ni-Co and Ni-Fe NBBs before spray-drying. Both of the NBBs exhibits a high homogeneity in diameter and shape suggesting that metal cations are homogeneously distributed in single particle rather

than segregation of hydroxide components in the nm-scale. Indeed, it is known that the divalent metal ions of Mn, Co, and Cu form layered hydroxide phases similar to α -Ni(OH)₂ and they are able to form solid solutions [35]. Generally, the replacement of Ni(II) with a trivalent metal in the preparation step of Ni-based hydroxides results in the segregation of trivalent metal (oxy)hydroxide because solubility products of M(III) and Ni(II) hydroxides are considerably different [36,37]. On the other hand, the present Ni-M layered double hydroxides form without any apparent segregation of M(III) hydroxides, which is suggested by a high homogeneity in diameter of NBBs for respective samples (Figure S2a-d). The chemical compositions obtained from STEM-EDS reveals that NBB contains Ni and substituted metal elements with molar ratio of Ni:M = 0.71–0.82:0.29–0.18 (Table S1). For all the systems, D_{NBB} was 2.05–3.24 nm, which are enough small toward formation of templated mesostructures. The macro- and mesostructures of heat-treated MMSs prepared from these various NBBs were shown in Figure 8d-g and S2e-l. The micrometer-scale spherical shape with dimple patterns were observed by SEM. TEM images revealed that the mesoporous structures were formed for all the samples. These results confirm that the synthesized crystals successfully worked as NBB to form mesostructure with F127 template and the obtained mesostructures were robust enough toward heat-treatment irrespective of the chemical composition. The chemical compositional versatility is important to improve and optimize the electrochemical, catalytic and magnetic properties of layered hydroxides [38-40].

In conclusion, the metal hydroxide MMSs with various diameter, surface structure, and chemical composition were successfully synthesized by epoxide-mediated alkalization and spray-drying. It is interesting to remark that the control of the sol-gel condensation conditions as well as the surface philicity permits to generate NBBs with adequately small sizes and interactions that generate self-assembled MMSs akin to those obtained in NBB-based mesoporous thin films [22]. An adequate understanding of these critical sizes and interactions can lead to the actual design of these complex materials with highly tailored porosity and wall structure [41].

Conclusion

Templated MMSs of nickel-based layered hydroxides were synthesized by spray-drying the NBBs which were prepared through the epoxide-mediated alkalization process in the presence of glutaric or acrylic acids. Reaction time and molar ratio, F127/Ni, were essential parameters to inhibit the formation of coarse crystal and macro phase separation between NBB and F127, allowing the successful assembly-formation of ordered MMS composed of α -Ni(OH)₂ NBBs. The diameter and surface texture of microspheres were controlled as 0.808 ± 0.196 – 1.49 ± 0.261 μm and from smooth surface to dimple patterned surface with a reaction parameter of the gas flow rate during spray-drying. NBBs of various chemical compositions were prepared

with the diameter about 2–3 nm through the same alkalization process by the partial replacement of nickel salt with target metal salts. Thus synthesized NBBs of various chemical compositions were successfully self-assembled into MMSs. Further understanding of these NBBs would open up the design of complex materials with highly tailored porosity and wall structure as well as high functionalities of layered nanocrystals.

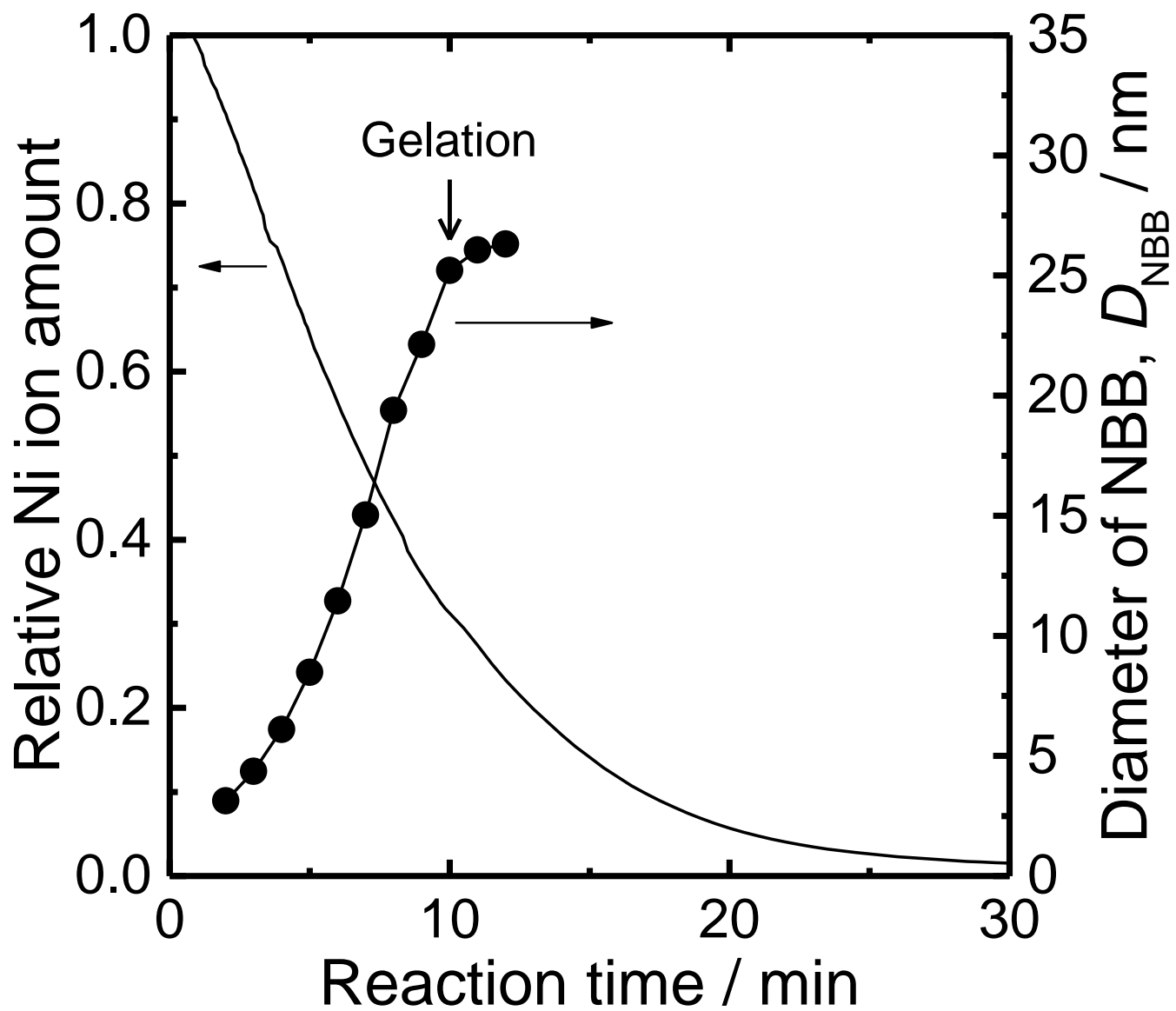


Figure 1. Time-dependence of relative Ni ion amount in the reacting solution (solid line) and the diameter of NBB calculated from in-situ SAXS patterns (close circle).

		T_r / min (Residual Ni ion)			
		1 (98.9%)	2 (90.7%)	5 (64.4%)	8 (42.4%)
F127/Ni	0.030		×	×	
	0.016	×	×	×	○
	0.005	×	×	○	○

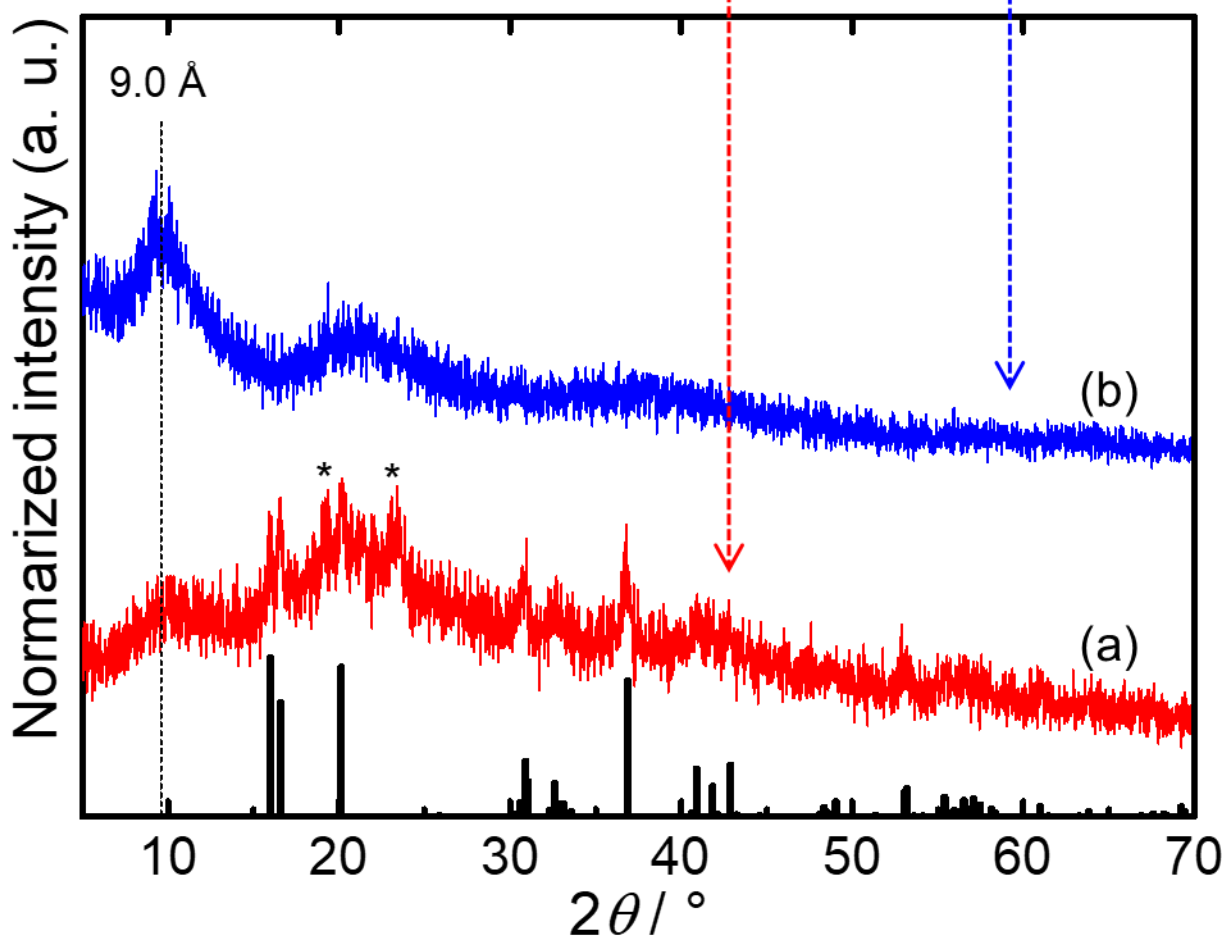


Figure 2. Effects of reaction time, t , and molar ratio of F127/Ni on the formed crystalline phase (×: α -Ni(OH)₂ with impurities and ○; pure α -Ni(OH)₂). Corresponding PXRD patterns of spray-dried powder prepared with different conditions; (a) $t = 2$ min, F127/Ni = 0.016, spray gas flow rate of 473 L/h, and (b) $t = 5$ min, F127/Ni = 0.005 spray gas flow rate of 742 L/h. (Black bar: NiCl₂·2H₂O (#72-0044)).

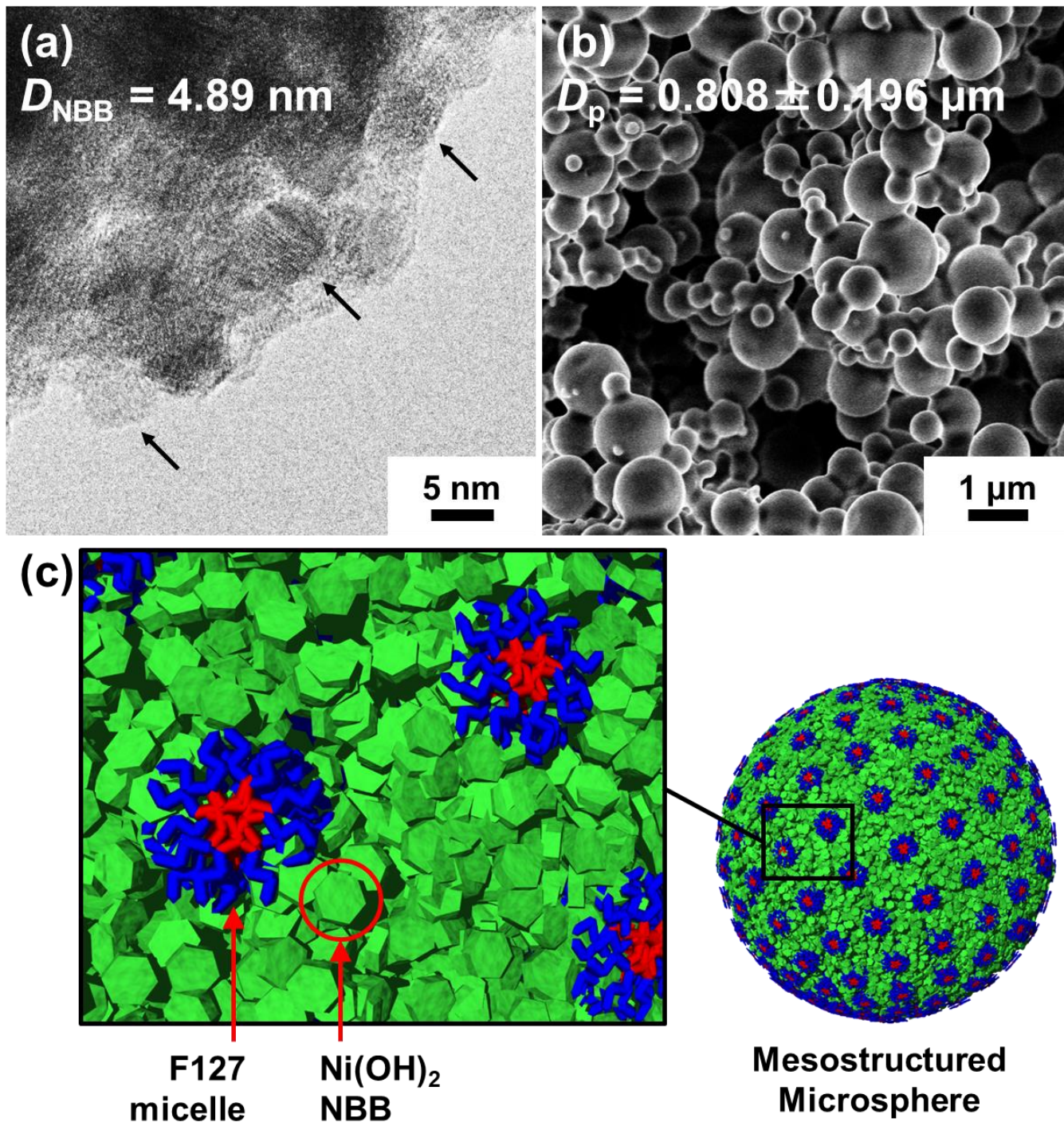


Figure 3. (a) TEM image of the NBB observed by drying the colloid on a TEM grid at $t = 5$ min. Black arrows indicate NBBs with a spherical shape. (b) SEM images of spray-dried MMS prepared with gas flow rate of 742 L/h. The condition of solution before spray-drying was $t = 5$ min and F127/Ni = 0.005. (c) Schematic illustration of spray-dried MMS composed of Ni(OH)₂ NBBs and F127 micelles.

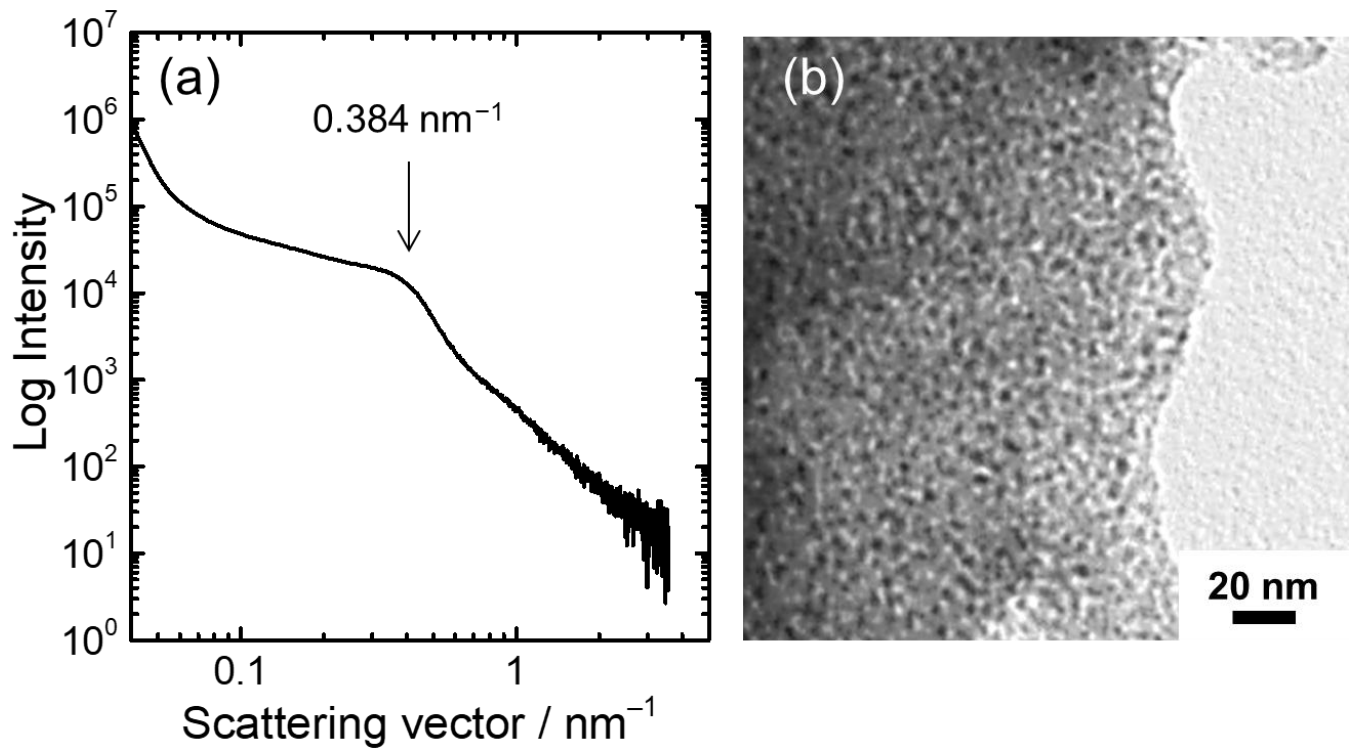


Figure 4. (a) SAXS pattern and (b) TEM image of heat-treated MMS prepared with gas flow rate of 742 L/h. The condition of solution before spray-drying was $t = 5$ min and F127/Ni = 0.005.

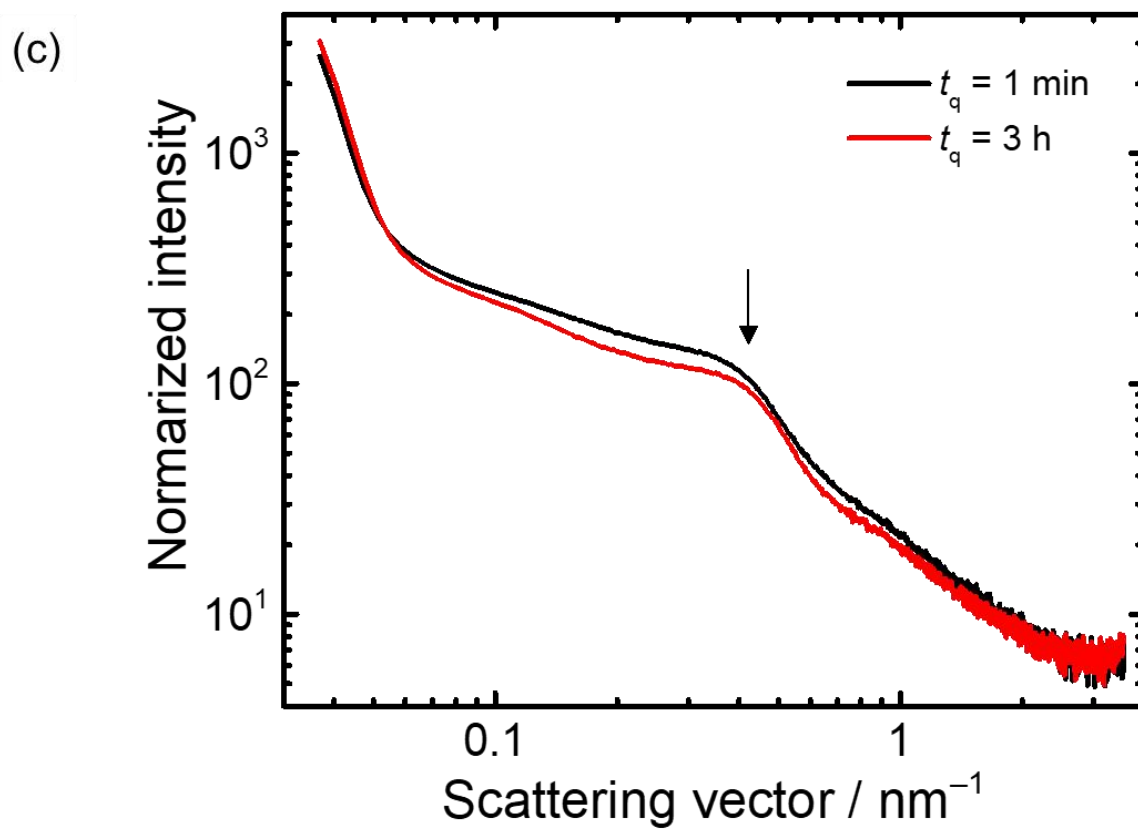
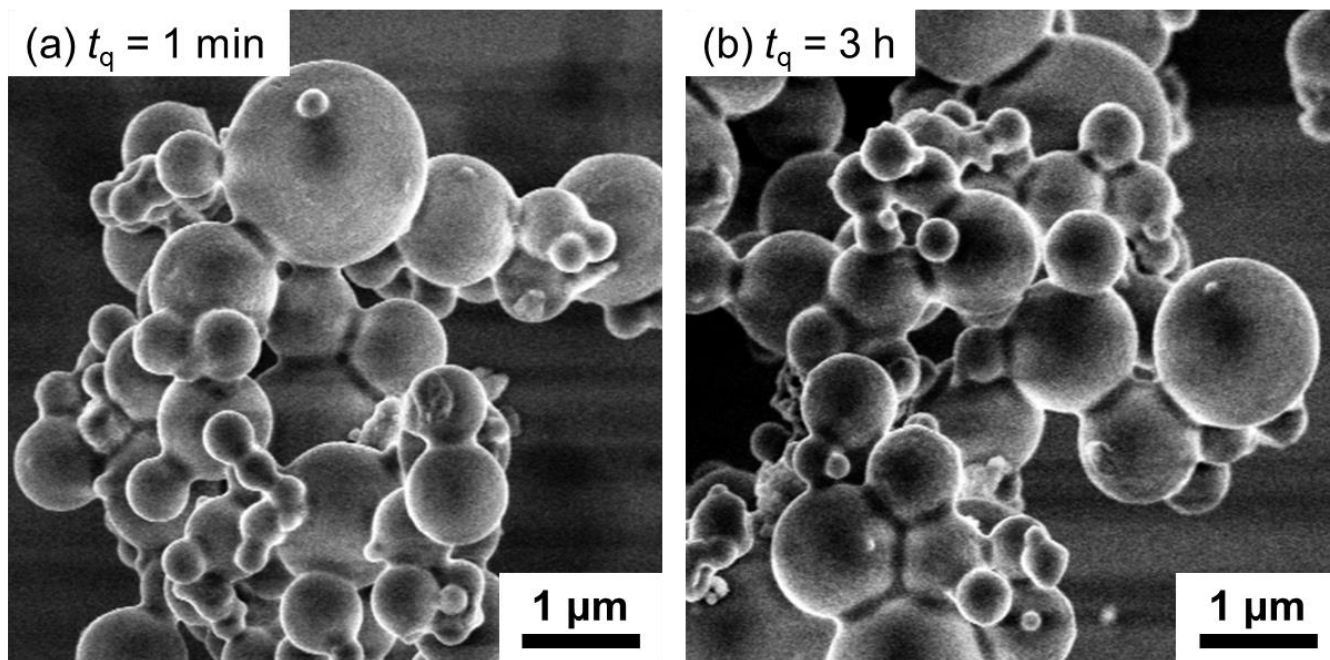


Figure 5. SEM images of spray-dried MMS prepared at different quenching time, t_q , of (a) 1 min and (b) 3 h. (c) SAXS patterns of spray-dried MMS prepared at $t_q = 1 \text{ min}$ (black) and 3 h (red). The arrow indicates the peaks corresponding to self-assembled meso-periodic structure of NBB and F127 micelles. The condition of solution before spray-drying was $t = 5 \text{ min}$ and $\text{F127/Ni} = 0.005$.

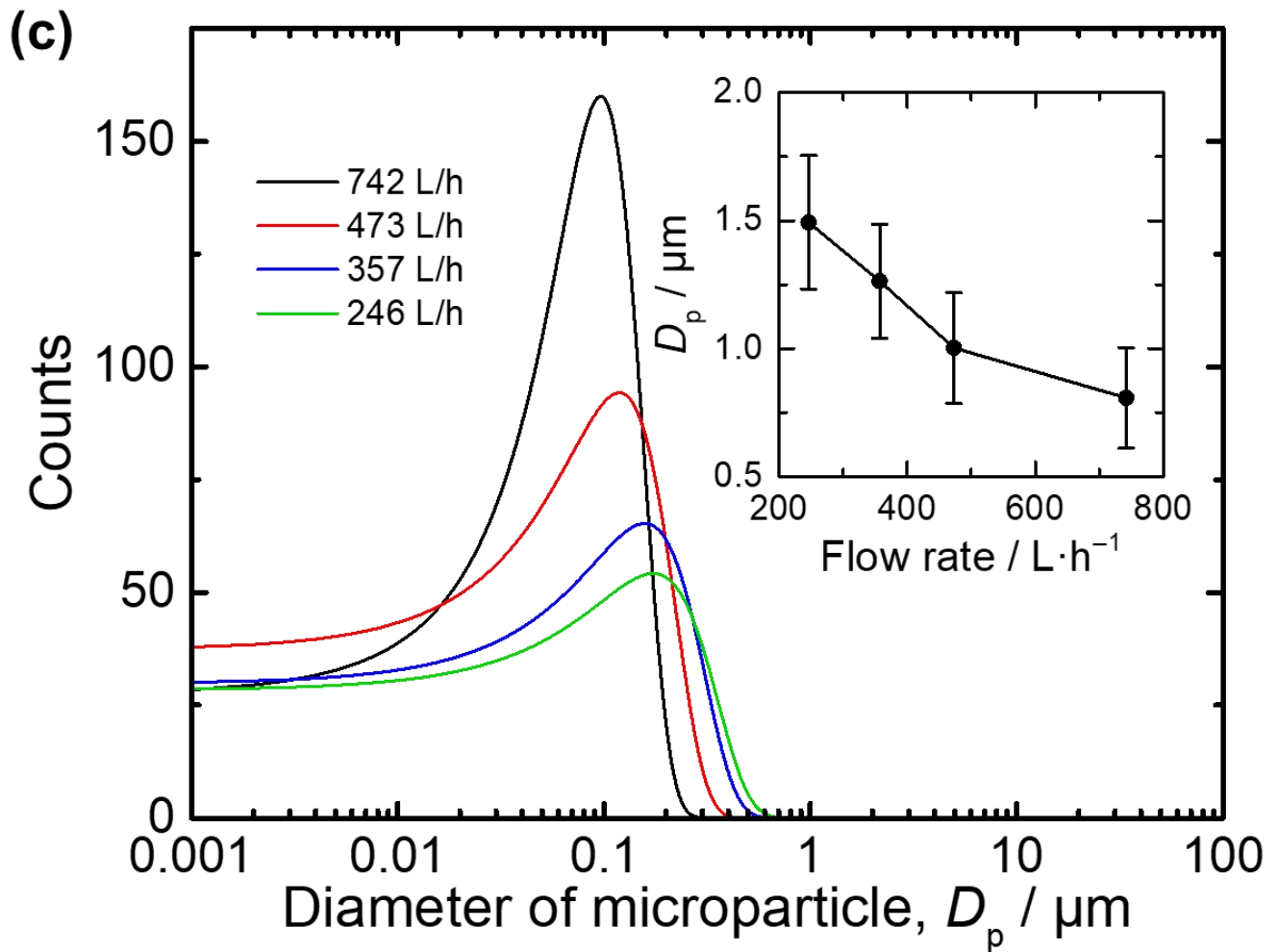
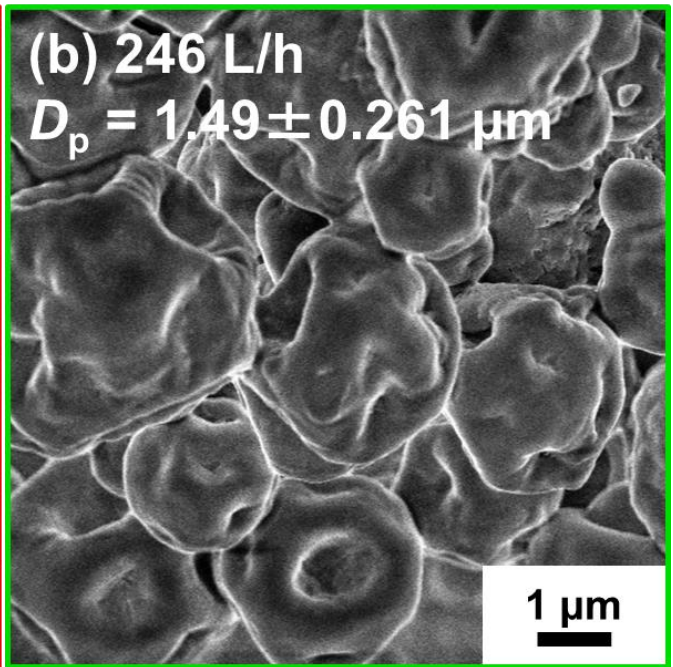
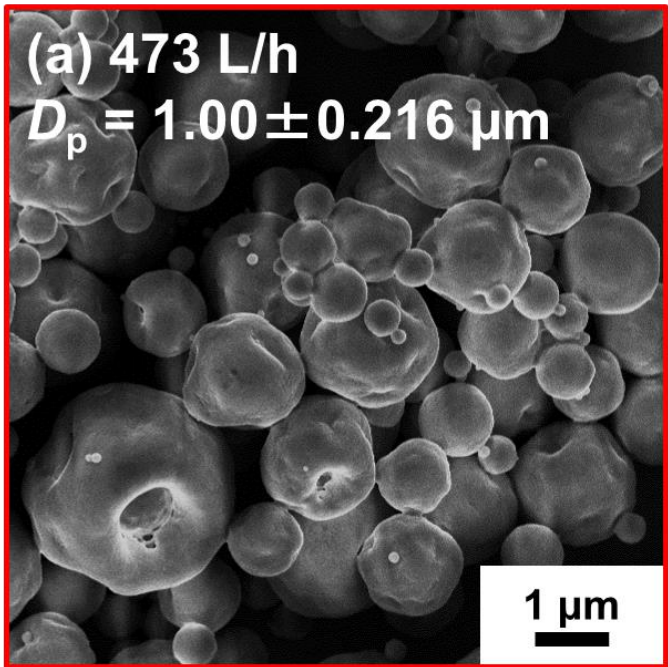


Figure 6. SEM images of spray-dried powders prepared with different gas flow rate of: (a) 473 L/h and (b) 246 L/h. (c) Particle size distribution curves (calculated from histogram) of MMSs prepared with different gas flow rate. The condition of solution before spray-drying was $t = 5$ min and $F_{127}/Ni = 0.005$ for all the samples. The diameters of 350 particles were averaged to estimate D_p for each sample. Inset of (c) is relationship between D_p and flow rate.

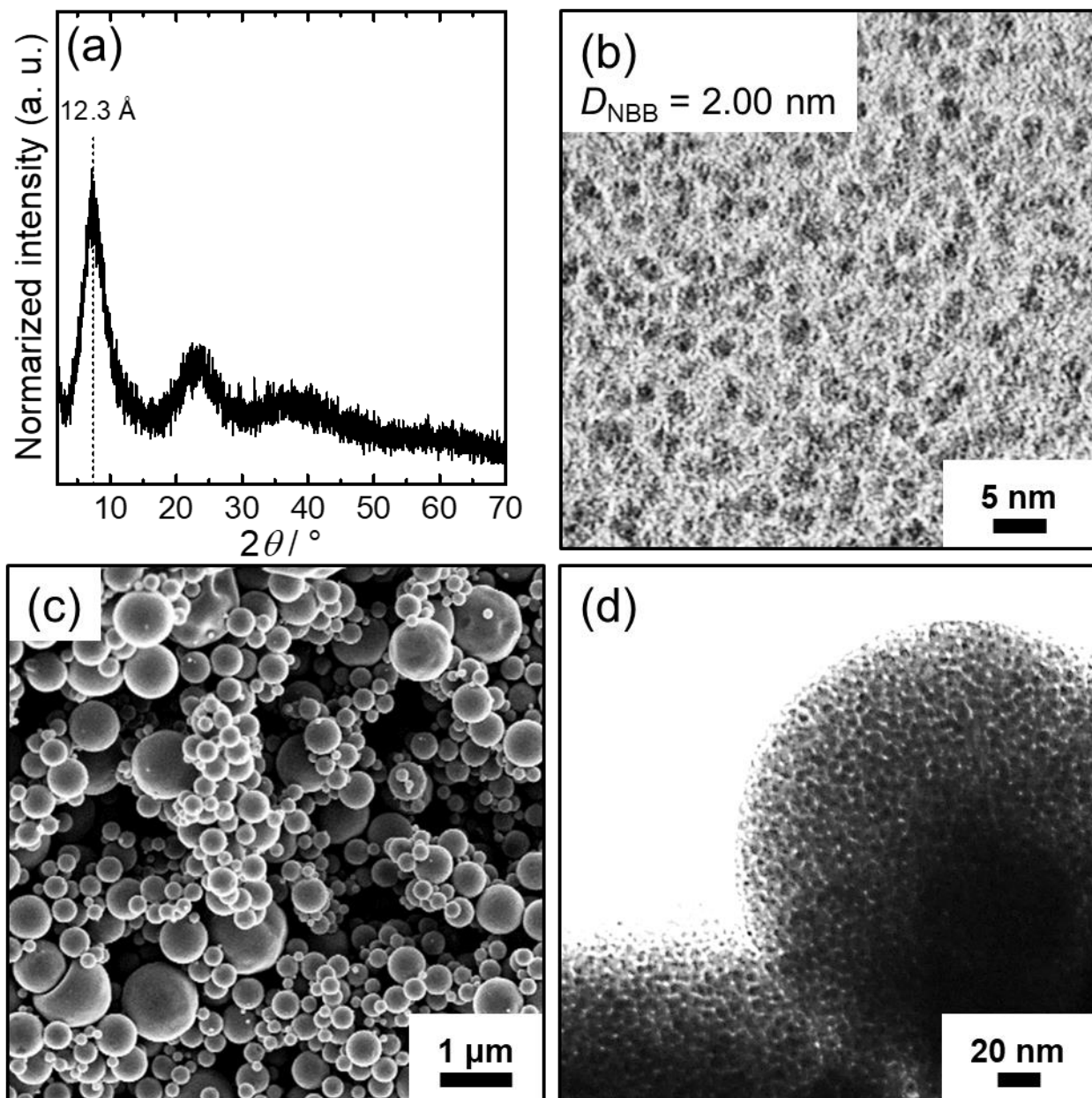
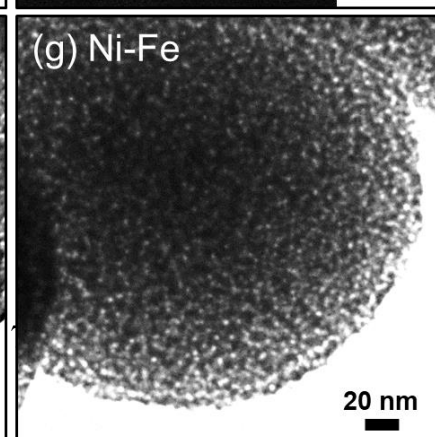
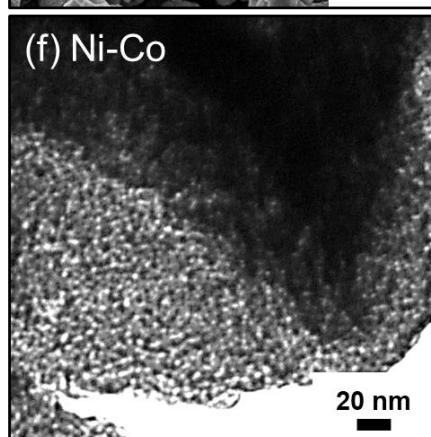
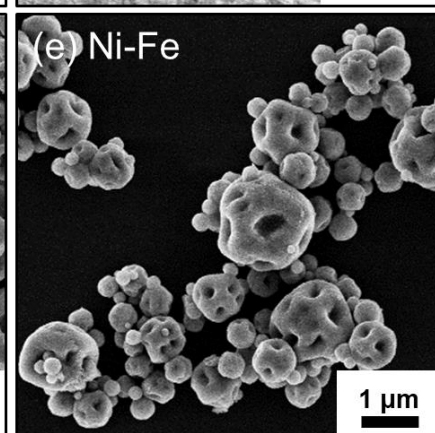
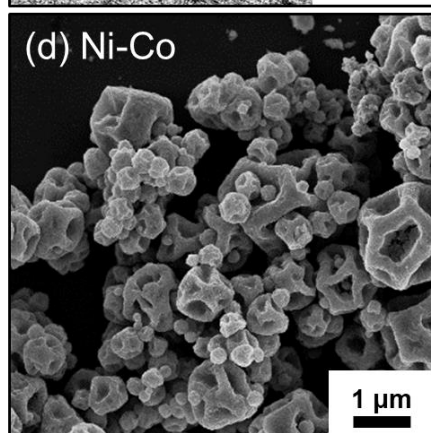
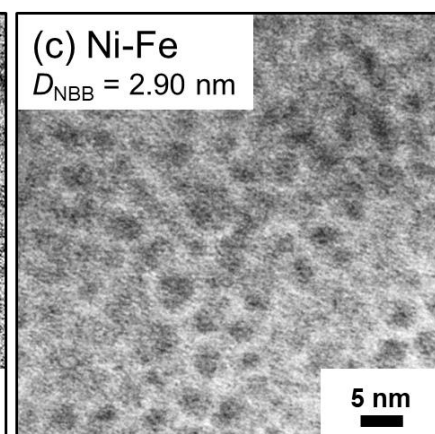
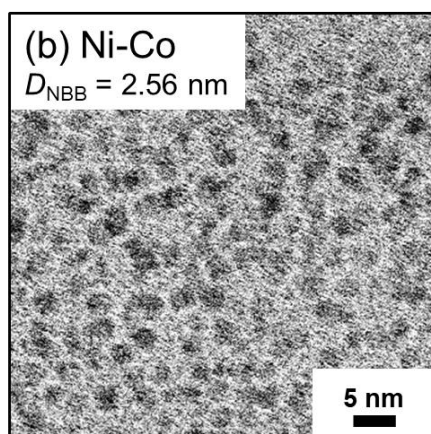
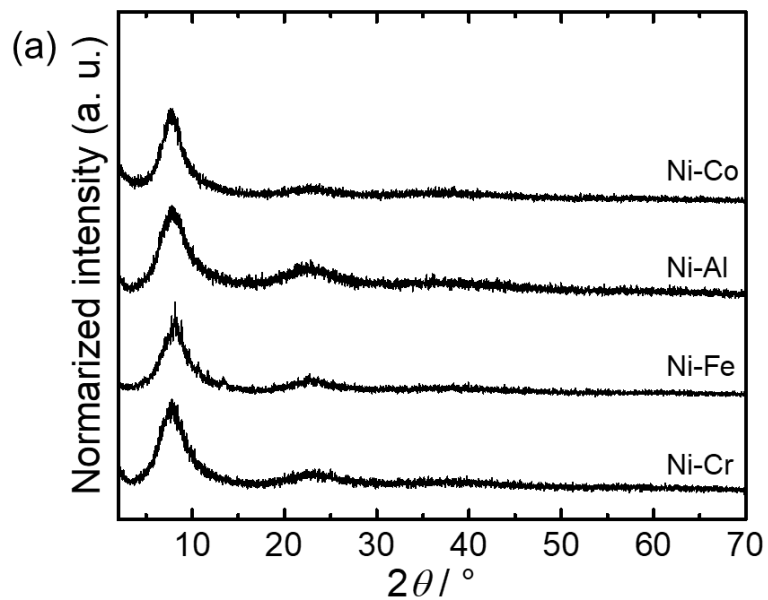


Figure 7. (a) PXRD pattern of spray-dried MMS, (b) STEM image of NBB before spray-drying, (c) SEM image and (d) TEM image of heat-treated MMS prepared from the solution including acrylic acid. The diameters of 100 particles were averaged to estimate D_{NBB} .



| Figure 8. (a) PXRD pattern of spray-dried MMSs, (b)(c) STEM image of NBBs used for spray-drying, (d)(e) SEM images and (f)(g) TEM images of heat-treated MMSs of Ni-M (M = Co(II) and Fe(III)). The diameters of 100 particles were averaged to estimate D_{NBB} .

ASSOCIATED CONTENT

Supporting Information. [PXRD pattern](#), [SEM](#), [TEM](#), [STEM](#) images and ~~time dependent Ni ion amount and NBB diameter~~[chemical composition of synthesized MMSs](#).

Present address of NT: Department of Chemical Science and Technology, Faculty of Bioscience and Applied Chemistry, Hosei University, Koganei, Tokyo 184-8584, Japan

ACKNOWLEDGMENT

Strategic Young Researcher Overseas Visits Program for Accelerating Brain Circulation from JSPS is gratefully acknowledged. The present work was partially supported by JSPS KAKENHI, JSPS bilateral program, LNLS proposal SAXS1 18927, ANPCyT (PICT 2012-2087 and 2015-3526), UBACyT (20020130100610BA), Hitachi Metals Materials Science Foundation, The Sumitomo Foundation, and Izumi Science and Technology Foundation. We thank Mr. J. Daniels and Mr. S. M. Nikka for the helpful discussions.

Compliance with ethical standards

Conflict of interest The authors declare that they have no conflict of interest.

REFERENCES

- (1) Arcos D, López-Noriega A, Ruiz-Hernández E, Terasaki O, Vallet-Regí M (2009) Chem Mater 21:1000-1009
- (2) Son HY, Kim KR, Lee JB, Kim THL, Jang J, Kim SJ, Yoon MS, Kim JW, Nam YS (2017) Sci Rep 7:14728
- (3) Liu Y, Lan K, Bagabas AA, Zhang P, Gao W, Wang J, Sun Z, Fan J, Elzatahry AA, Zhao D (2016) Small 12:860-867.
- (4) Hou S, Li X, Wang H, Wang M, Zhang Y, Chi Y, Zhao Z (2017) RSC Adv 7:51993-52000
- (5) Zhou J, Wang Y, Wang J, Qiao W, Long D, Ling L (2016) J Colloid Interface Sci 462:200-207
- (6) Hassan MS, Lau RWM (2009) AAPS PharmSciTech 1-:1252-1262
- (7) Liu Y, Shen D, Chen G, Elzatahry AA, Pal M, Zhu H, Wu L, Lin J, Al-Dahyan D, Li W, Zhao D (2017) Adv Mater 29:1702274
- (8) Cirujano FG, Luz I, Soukri M, Goethem CV, Vankelecom IFJ, Lail M, Vos DED (2017) Angew Chem Int Ed 56:13302-13306
- (9) Meng FL, Wang ZL, Zhong HX, Wang J, Yan JM, Zhang XB (2016) Adv Mater 28:7948–7955
- (10) Tian M, Sun Y, Zhang CJ, Wang J, Qiao W, Ling L, Long D (2017) J Power Sources 364:182-190
- (11) Shi Y, Wan Y, Zhao D (2011) Chem Soc Rev 40:3854-3878
- (12) Gu D, Schüth F (2014) Chem Soc Rev 43:313-344
- (13) Griin M, Lauer I, Unger KK (1997) Adv Mater 9:254-257
- (14) Lu Y, Fan H, Stump A, Ward TL, Rieker T, Brinker CJ (1999) Nature 398:223-226

- (15) Grosso D, Soler-Illia GJAA, Crepaldi EL, Charleux B, Sanchez C (2003) *Adv Funct Mater* 13:37-42
- (16) Sanchez C, Soler-Illia GJAA, Ribot F, Lalot T., Mayer CR, Cabuil V (2001) *Chem Mater* 13:3061-3082
- (17) Fan J, Boettcher SW, Stucky GD (2006) *Chem Mater* 18:6391-6396
- (18) Boettcher SW, Fan J, Tsung CK, Shi Q, Stucky GD (2007) *Acc Chem Res* 40:784-792
- (19) Boissiere C, Grosso D, Chaumonnot A, Nicole L, Sanchez C (2010) *Adv Mater* 23:599-623
- (20) Gash AE, Tillotson TM, Satcher JH, Poco JF, Hrubesh LW, Simpson RL (2001) *Chem Mater* 13:999-1007
- (21) Tokudome Y, Tarutani N, Nakanishi K, Takahashi M (2013) *J Mater Chem A* 1:7702-7708
- (22) Tarutani N, Tokudome Y, Jobbágy M, Viva FA, Soler-Illia GJAA, Takahashi M (2016) *Chem Mater* 28:5606-5610
- (23) Wong MS, Jeng ES, Ying JY (2001) *Nano Lett* 1:637-642
- (24) Rauda IE, Buonsanti R, Saldarriaga-Lopez LC, Benjauthrit K, Schelhas LT, Stefik M, Augustyn V, Ko J, Dunn B, Wiesner U, Milliron DJ, Tolbert SH (2012) *ACS Nano* 6:6386-6399
- (25) Warren SC, Messina LC, Slaughter LS, Kamperman M, Zhou Q, Gruner SM, DiSalvo FJ, Wiesner U (2008) *Science* 320:1748-1752
- (26) Soler-Illia GJAA, Scolan E, Louis A, Albouyb PA, Sanchez C (2001) *New J Chem* 25:156-165
- (27) Innocenzi P, Luca Malfatti L, Piccinini M, Marcelli A (2010) *J Phys Chem A* 114:304-308
- (28) Zhao D, Feng J, Huo Q, Melosh N, Fredrickson GH, Chmelka BF, Stucky GD (1998) *Science* 279:548-552
- (29) Soler-Illia GJAA, Sanchez C, Lebeau B, Patarin J (2002) *Chem Rev* 102:4093-4138
- (30) Pauly TR, Liu Y, Pinnavaia TJ, Billinge SJL, Rieker TP (1999) *J Am Chem Soc*, 121:8835-8842
- (31) Kudas TT, Hampden-Smith MJ (1999) *Aerosol Processing of Materials*. John Wiley & Sons, New York
- (32) Olhero SM, Ferreira JMF (2004) *Powder Technol* 139:69-75
- (33) Mueller S, Llewellyn EW, Mader HM (2011) *Geophys Res Lett* 38:L13316
- (34) Vaysse C, Guerlou-Demourgues L, Duguet E, Delmas C (2003) *Inorg Chem* 42:4559-4567
- (35) Arizaga GGC, Satyanarayana KG, Wypych F (2007) *Solid State Ionics* 178:1143-1162
- (36) Bocclair JW, Braterman PS (1999) *Chem Mater* 11:298-302
- (37) Tarutani N, Tokudome Y, Fukui M, Nakanishi K, Takahashi M (2015) *RSC Adv* 5:57187-57192
- (38) Nguyen T, Boudard M, Carmezim MJ, Montemor MF (2017) *Energy* 126:208-216
- (39) Song F, Hu X (2014) *Nat Commun* 5:4477
- (40) Abellán G, Carrasco JA, Coronado E (2013) *Inorg Chem* 52:7828-7830
- (41) Tang Q, Angelomé PC, Soler-Illia GJAA, Müller M (2017) *Phys Chem Chem Phys* 19:28249-28262
-